

# Regulation of Nerve Growth Mediated by Inositol 1,4,5-Trisphosphate Receptors in Growth Cones

Kohtaro Takei,\* Ryong-Moon Shin, Takafumi Inoue, Kunio Kato, Katsuhiko Mikoshiba

The inositol 1,4,5-trisphosphate (IP<sub>3</sub>) receptor (IP<sub>3</sub>R) acts as a Ca<sup>2+</sup> release channel on internal Ca<sup>2+</sup> stores. Type 1 IP<sub>3</sub>R (IP<sub>3</sub>R1) is enriched in growth cones of neurons in chick dorsal root ganglia. Depletion of internal Ca<sup>2+</sup> stores and inhibition of IP<sub>3</sub> signaling with drugs inhibited neurite extension. Microinjection of heparin, a competitive IP<sub>3</sub>R blocker, induced neurite retraction. Acute localized loss of function of IP<sub>3</sub>R1 in the growth cone induced by chromophore-assisted laser inactivation resulted in growth arrest and neurite retraction. IP<sub>3</sub>-induced Ca<sup>2+</sup> release in growth cones appears to have a crucial role in control of nerve growth.

In developing and regenerating neurons, the growth cone located at a distal tip of a neurite is thought to be the site governing nerve growth and axon guidance (1). Ca<sup>2+</sup> is implicated in various signaling pathways in nerve growth and growth cone behavior (2, 3). An optimal range of the concentration of intracellular Ca<sup>2+</sup> ([Ca<sup>2+</sup>]<sub>i</sub>) in growth cones is required for proper nerve growth (2). Transient increase of [Ca<sup>2+</sup>]<sub>i</sub> in the growth cone is a key step in the signaling cascade for laminin-mediated growth cone navigation (4), cell adhesion-mediated neurite extension (5), growth cone migration (6), and axon turning (7). This transient increase of [Ca<sup>2+</sup>]<sub>i</sub> is thought to be caused by Ca<sup>2+</sup> influx across the plasma membrane through Ca<sup>2+</sup> channels such as the L-type voltage-dependent Ca<sup>2+</sup> channel (8). IP<sub>3</sub> triggers release of Ca<sup>2+</sup> from internal Ca<sup>2+</sup> stores into the cytosol through the IP<sub>3</sub>R. Whether IP<sub>3</sub> signaling and IP<sub>3</sub>-induced Ca<sup>2+</sup> release (IICR) are involved in nerve growth has not been determined.

The IP<sub>3</sub>R1, a major neuronal member of the IP<sub>3</sub>R family, is highly expressed in the Purkinje neurons of the mouse cerebellum (9). IP<sub>3</sub>R1 was detected in chick dorsal root

ganglia (DRG) and cerebellum as determined by protein immunoblotting (10) (Fig. 1A). IP<sub>3</sub>R1 was primarily detected by immunocytochemistry (11) in the central domain of the growth cone and along the neurite of chick DRG neurons (Fig. 1B).

We characterized the effects of thapsigargin (TG) [which blocks Ca<sup>2+</sup>-adenosine 5'-triphosphatase (Ca<sup>2+</sup>-ATPase) on the endoplasmic reticulum and eventually depletes intracellular Ca<sup>2+</sup> stores (12)] on neurite extension of chick DRG neurons cultured on laminin (13). Application of TG (10 μM) for 2 hours significantly inhibited neurite extension (*P* < 0.01) (Fig. 2A). Wash-out of TG

resulted in recovery of the extension rate to that of untreated neurites (Fig. 2B). To distinguish effects of TG on neurite extension from those on neuritogenesis (which means initiation of neurite formation), we delayed drug treatments until 2 hours after the cells had been plated. This delayed treatment shifted the neurite length distribution and significantly inhibited the median neurite length 2 hours after addition of TG (Fig. 2C). Therefore, blockage of the TG-sensitive Ca<sup>2+</sup> uptake in internal stores appears to inhibit neurite extension.

We also examined the effect of lithium ion and heparin, a competitive IP<sub>3</sub>R blocker, on neurite extension (13, 14). Lithium is assumed to block the recycling of IP<sub>3</sub> into inositol by inhibiting the hydrolysis of intermediate inositol phosphates, and this compound eventually results in loss of the IP<sub>3</sub> signal (15). Exposure of cells to LiCl (50 mM) for 2 hours significantly inhibited neurite extension (Fig. 2D). In DRG neurons loaded with heparin by trituration (14), the neurite extension rate was significantly inhibited (Fig. 2D). The heparin analog, de-*N*-sulfated heparin, had no effect. TG, lithium, and heparin had no effect on growth cone morphology. We microinjected heparin or de-*N*-sulfated heparin into the cell body of DRG neurons and observed growth cone behavior by time-lapse video microscopy (16). Microinjection of heparin but not the control analog resulted in growth arrest of neurites and subsequent neurite retraction with bending (Fig. 2E, Table 1). Motility of filopodia was unaffected by heparin (Table 1). Because TG, lithium, and heparin had inhibitory effects on neurite extension, IP<sub>3</sub> signaling and

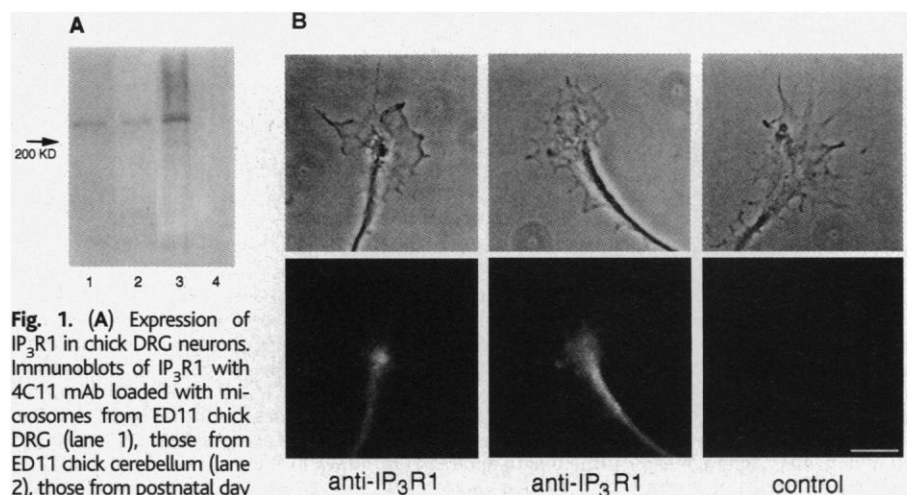


**Fig. 1.** (A) Expression of IP<sub>3</sub>R1 in chick DRG neurons. Immunoblots of IP<sub>3</sub>R1 with 4C11 mAb loaded with microsomes from ED11 chick DRG (lane 1), those from ED11 chick cerebellum (lane 2), those from postnatal day (PD) 20 mouse cerebellum (positive control) (lane 3), and those from PD20 IP<sub>3</sub>R1 knockout mouse cerebellum (negative control) (lane 4) (29). Immunodetection in all samples probed with nonspecific rat IgG was nil. (B) Distribution of IP<sub>3</sub>R1 in chick DRG neurons cultured on laminin. Phase-contrast images in top panels correspond to fluorescence images in bottom panels. Indirect immunofluorescence with 4C11 mAb is shown as anti-IP<sub>3</sub>R1. An experiment with nonspecific rat IgG is shown as a control. Other control experiments that omitted primary antibodies and probed with secondary antibodies gave completely negative results. Scale bar, 5 μm.

K. Takei and K. Kato, Calciosignal Net Project, Exploratory Research for Advanced Technology (ERATO), Japan Science and Technology Corporation (JST), Bunkyo-Ku, Tokyo 113-0021, Japan. R.-M. Shin and T. Inoue, Department of Molecular Neurobiology, Institute of Medical Science, University of Tokyo, Minato-Ku, Tokyo 108-0071, Japan. K. Mikoshiba, Calciosignal Net Project, ERATO, JST, Bunkyo-Ku, Tokyo 113-0021, Japan, Department of Molecular Neurobiology, Institute of Medical Science, University of Tokyo, Minato-Ku, Tokyo 108-0071, Japan, and Brain Science Institute, RIKEN, Wako, Saitama 351-0198, Japan.

\*To whom correspondence should be addressed. E-mail: kohtaro@ims.u-tokyo.ac.jp

## REPORTS

IP<sub>3</sub>R functions are implicated in neurite extension.

To examine functions of IP<sub>3</sub>R in regions of the growth cone, we used the chromophore-assisted laser inactivation (CALI) technique, a method of protein ablation that has high spatial and temporal specificity (17–21). CALI uses laser irradiation to direct spatially restricted photogenerated hydroxyl free radical damage to targeted proteins through chromophore (malachite green, MG)-conjugated antibodies (18), thereby allowing one to inactivate protein function preferentially without affecting other cellular functions (17, 19–21). We used microscale CALI (micro-CALI) to test whether IP<sub>3</sub>R1 in the growth cone would potentiate nerve growth regulation. Effects of CALI of IP<sub>3</sub>R1 on IICR activity in vitro were measured with a luminescence spectrometer and the mouse cerebellum microsomes fraction, in which the IP<sub>3</sub>R1 is specifically concentrated (9, 22). The 4C11 monoclonal antibody (mAb) itself blocks neither IP<sub>3</sub> binding nor Ca<sup>2+</sup> release from microsomes (23). CALI of IP<sub>3</sub>R1 with chromophore-labeled 4C11 mAb caused about a 50% reduction in IICR activity. This inactivation depended on both the presence of chromophore-labeled 4C11 mAb and laser irradiation (Fig. 3A). CALI with chromophore-labeled nonspecific immunoglobulin G (IgG) did not affect IICR

activity. CALI of IP<sub>3</sub>R1 had no inhibitory effect on Ca<sup>2+</sup> uptake activity by Ca<sup>2+</sup>-ATPase. Thus, CALI of IP<sub>3</sub>R1 causes a potent reduction of IICR activity in living cells.

We loaded chromophore-labeled 4C11 mAb or nonspecific IgG into DRG neurons by trituration, monitored loading of antibodies into neurites and growth cones by observ-

**Table 1.** Heparin microinjection and micro-CALI of IP<sub>3</sub>R1. Comparison of growth cone behavior with control experiments on phenotypes observed after heparin microinjection and micro-CALI of IP<sub>3</sub>R1 is shown. Growth arrest is defined as neurite extension after manipulation, a more than 90% reduction of the neurite extension rate before manipulation, and a transient neurite retraction within 5 min after manipulation. Neurite retraction is defined as neurite shown a decrease of its length by continuous retraction after manipulation. No phenotype was observed before microinjection of heparin and laser irradiation for CALI experiments, in all cases tested ( $n = 85$  in total). Comparison of neurite extension rate after CALI of IP<sub>3</sub>R1 (from +5 min to +10 min shown in Fig. 3, C, D, and E) with that before CALI (from –5 min to +0 min) is shown. Data shown are the averages of neurite extension rate and SEM (micrometers per 5 min).

	Treatment				
	Heparin injection	Heparin analog injection	CALI of IP <sub>3</sub> R1 in growth cones	CALI of IgG in growth cones	CALI of IP <sub>3</sub> R1 in neurite shafts
Number of cases	15	12	26	22	10
	<i>Frequency</i>				
Behavior					
Growth arrest	12/15*	3/12	19/26**	1/22	0/10
Neurite retraction	12/15*	3/12	14/26**	0/22	0/10
Neurite bending	12/15*	3/12	7/26	0/22	0/10
Filopodial retraction	0/15	0/12	0/26	0/22	0/10
	<i>Average neurite extension rate</i>				
Before CALI			+4.35 ± 1.21	+6.13 ± 1.10	+4.70 ± 3.02
After CALI			–3.60 ± 1.09***	+4.82 ± 1.32	+5.76 ± 2.70

\*,  $P < 0.05$ ; \*\*,  $P < 0.01$ , significantly associated with phenotypes, compared with findings in the control ( $\chi^2$  test); \*\*\*,  $P < 0.001$ , significantly different from neurite extension rate before CALI (Student's unpaired  $t$  test).

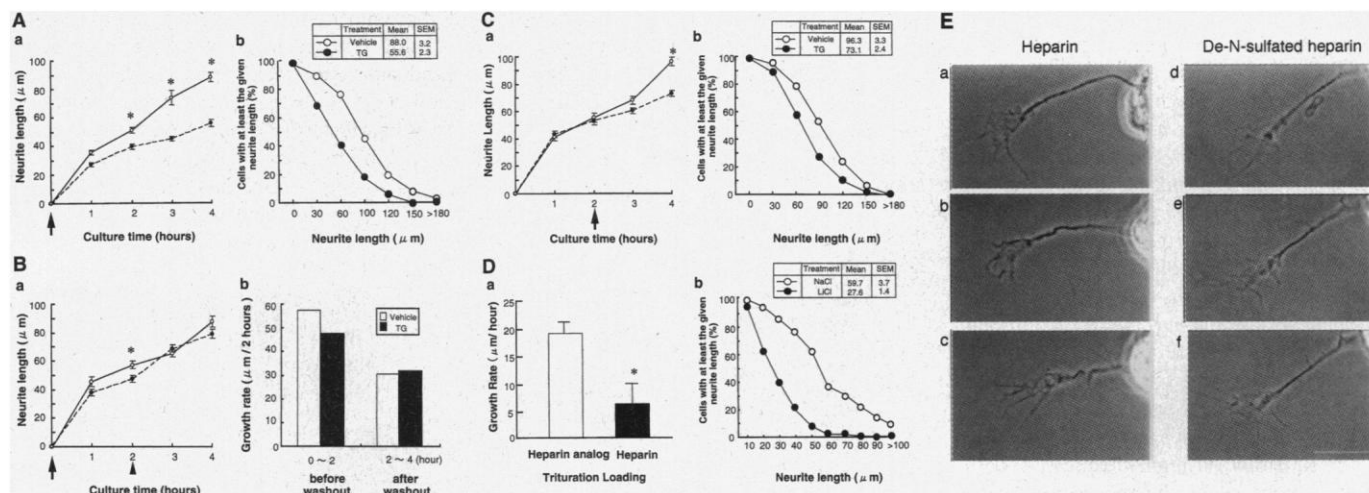


**Fig. 2.** Effects of inhibitors on neurite extension. (A) Effect of TG treatment. (a) Kinetics of neurite extension under TG (filled circles) or vehicle (open circles) treatments. TG was added at the time of plating (arrow). Data indicate mean neurite length and standard error of the mean (SEM). \*, significantly lower than vehicle at each time point;  $P < 0.01$  by Student's unpaired  $t$  test. (b) The distribution of DRG neurons with different neurite lengths under TG treatment (4 hours) is plotted as a cumulative histogram. Mean neurite length and SEM are shown in the inset table. Statistical analysis was by one-way analysis of variance (ANOVA), with all pairwise multiple comparison test (Tukey test). TG treatment is significantly different from control ( $P < 0.05$ ). (B) Wash-out of TG. (a) TG (filled circles) was added at the time of plating (arrow). DRG neurons were treated with TG for 2 hours and washed with culture medium (arrowhead). \*, significantly lower than vehicle at each time point;  $P < 0.01$  by Student's unpaired  $t$  test. (b) The averages of growth rate (neurite extension length/2 hours) before and after wash-out. (C) Effect of delayed TG treatment. (a) DRG neurons were treated with TG

2 hours after plating (arrow). (b) TG treatment for 2 hours is significantly different from control;  $P < 0.05$  by one-way ANOVA. (D) Effect of heparin and lithium. (a) Inhibition of neurite extension rate by heparin. Heparin was loaded by trituration, and the longest neurite of a cell loaded with heparin was measured at 2- and 3-hour culture time points, in the same cell. Data shown are average median growth rate (neurite extension length/hour) and SEM. \*, significantly lower than control reagents;  $P < 0.01$  by Student's unpaired  $t$  test. (b) LiCl treatment (filled circles) for 2 hours is significantly different from control (open circles);  $P < 0.05$  by one-way ANOVA. (E) Microinjection of heparin or a control analog, de-N-sulfated heparin. (a) A growth cone is observed before the microinjection. Viability of the growth cone was verified during this period. (b) The neurite begins to retract and bend after injection (15 min after injection). (c) Heparin injection results in neurite retraction with bending, but not filopodial retraction (30 min after injection). (d, e, and f) Microinjection of a control analog did not affect growth cone behavior. Scale bar, 10 μm.

## REPORTS

ing coincidental loading of fluorescein isothiocyanate (FITC)-conjugated dextran (molecular size: 150 kD) or FITC-labeled nonspecific IgG, and confirmed loading by immunocytochemistry (Fig. 3B). The region of interest was laser irradiated for 5 min, and the growth cone was observed by time-lapse video microscopy before, during, and after laser irradiation (24). Micro-CALI of IP<sub>3</sub>R1 in growth cones resulted in growth arrest of neurites and subsequent neurite retraction, within 5 min after termination of the irradiation (Fig. 3C). Growth arrest of neurites or neurite retractions were observed in 19 of 26 (73.1%) or 14 of 26 (53.8%) IP<sub>3</sub>R1 micro-CALI experiments (cells), respectively (Table 1;  $P < 0.01$  by  $\chi^2$  test). In 7 of 26 cases, the neurite retraction was accompanied by neurite bending (Fig. 3C, panel c, and Table

1). Filopodial motility was not affected (Fig. 3C and Table 1). In contrast, parallel micro-CALI experiments with chromophore-labeled nonspecific IgG showed no perturbation of growth cone behavior or neurite extension (Fig. 3E and Table 1). Laser irradiation alone toward the growth cone had no effect on growth cone behavior or neurite extension (Fig. 3E and Table 1). Neurite retraction appears not to be a nonspecific trauma response to CALI effects, because micro-CALI of calcineurin (19), myosin-V (20), talin (21), or vinculin (21) in growth cones causes various different phenotypes in filopodia but not in neurites. In contrast to the results of micro-CALI in growth cones, micro-CALI of IP<sub>3</sub>R1 in regions of the neurite shaft did not affect growth cone behavior (Fig. 3D and Table 1). This suggests that IP<sub>3</sub>R1 in growth cones has an important role

in neurite extension, whereas IP<sub>3</sub>R1 in neurite shafts is unlikely to function in neurite extension. The IP<sub>3</sub>R1 may need to be recruited to the growth cone to function with other signaling molecules.

Local loss of IP<sub>3</sub>R1 function within the growth cone results in growth arrest and neurite retraction, even though the neurons do undergo Ca<sup>2+</sup> influxes across the plasma membrane. Although a change in [Ca<sup>2+</sup>]<sub>i</sub> within the growth cone in response to inactivation of IP<sub>3</sub>R1 was not detectable in calcium imaging experiments with a fura-2 indicator (25), our findings do suggest that IICR within the growth cone, which may cause a small transient change in [Ca<sup>2+</sup>]<sub>i</sub>, is a key regulatory factor governing neurite extension. Although the molecular events downstream of Ca<sup>2+</sup> fluxes are not well understood in nerve

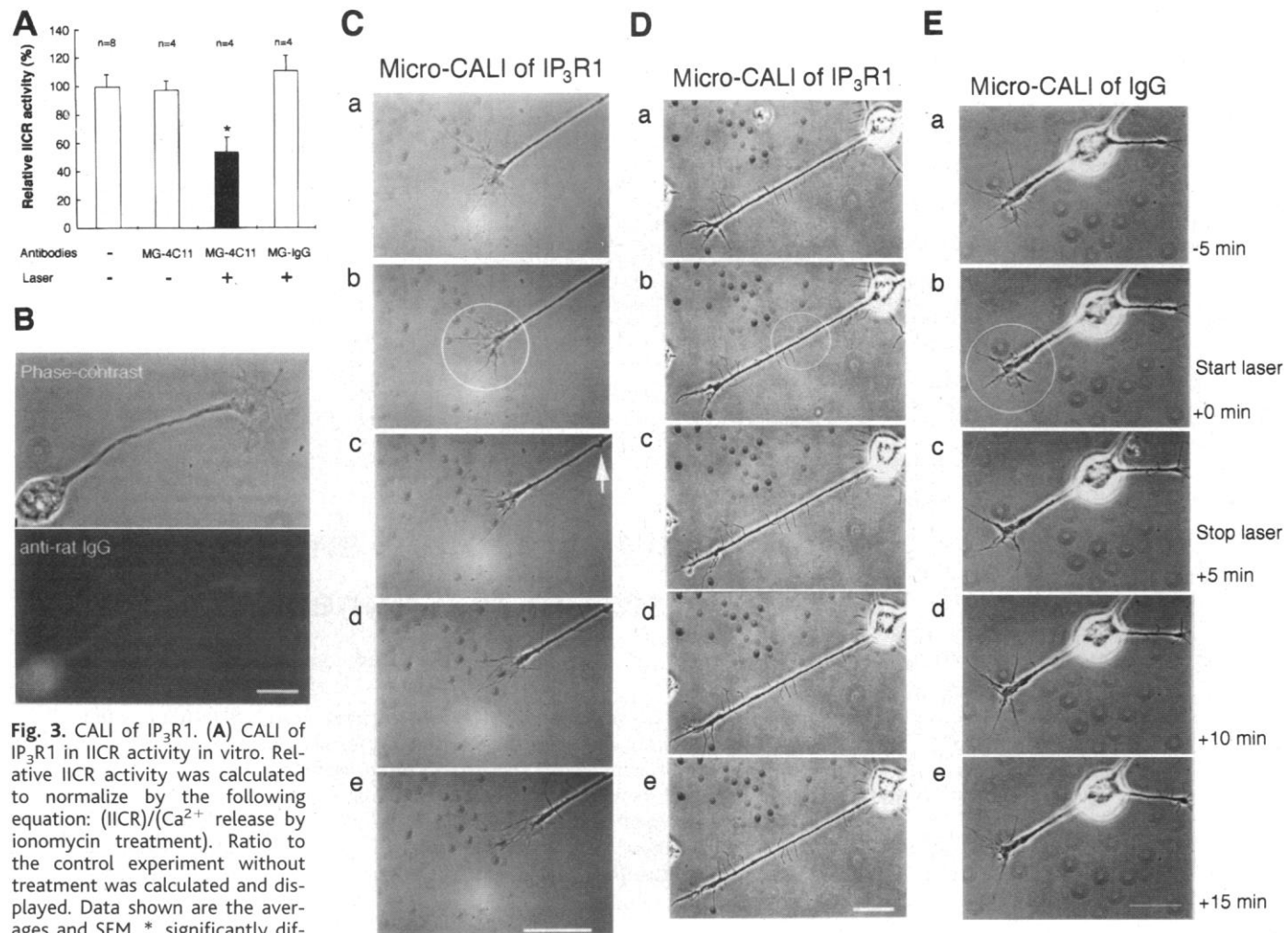


**Fig. 3.** CALI of IP<sub>3</sub>R1. **(A)** CALI of IP<sub>3</sub>R1 in IICR activity in vitro. Relative IICR activity was calculated to normalize by the following equation: (IICR)/(Ca<sup>2+</sup> release by ionomycin treatment). Ratio to the control experiment without treatment was calculated and displayed. Data shown are the averages and SEM. \*, significantly different from all control groups;  $P < 0.02$  by Student's unpaired  $t$  test. **(B)** Trituration loading of chromophore (MG)-labeled 4C11 mAb was confirmed by immunocytochemistry with a secondary antibody (2 hours of culture after trituration). Unloaded neurons were not stained. Scale bar, 5  $\mu$ m. **(C)** Micro-CALI of IP<sub>3</sub>R1 in growth cone. Sequential panels from top to bottom show the time course of growth cone behavior during the observation (every 5 min). (a) A growth cone is first observed for 5 min before laser irradiation (from -5 min to +0 min). (b) A region of

growth cone is chosen for micro-CALI (white outline: laser spot) and laser irradiated for 5 min (from +0 to +5 min). (c) The neurite stalls and starts retracting after laser irradiation (+5 min). Neurite bending also appears (arrow). (d and e) Neurite is retracting, whereas filopodia are not retracting (from +10 to +15 min). **(D)** Micro-CALI of IP<sub>3</sub>R1 in neurite shaft does not affect neurite extension. **(E)** Control micro-CALI with MG-nonspecific IgG (micro-CALI of IgG) in growth cone has no effect. Scale bars in (C), (D), and (E), 10  $\mu$ m.

growth, calmodulin (CaM) (26), an intracellular  $Ca^{2+}$  receptor protein; calcineurin (19), a CaM-dependent protein phosphatase; and  $Ca^{2+}$ -CaM-dependent protein kinase II (27) regulate nerve growth. Double immunostaining of  $IP_3R1$  and microtubules revealed that the distribution of  $IP_3R1$  was associated with that of microtubules such as tubulin in the growth cone (28). Thus, IICR through  $IP_3R1$  in the growth cone and its downstream effectors might act locally to regulate microtubule assembly and promote neurite extension. This notion is also supported by our findings that  $IP_3R1$  appears not to be distributed in filopodia and that inactivation of this molecule does not affect filopodial motility.  $[Ca^{2+}]_i$  mobilization by IICR could modulate  $Ca^{2+}$  influxes through  $Ca^{2+}$  channels. Therefore, IICR from internal stores and  $Ca^{2+}$  influx may act together to direct nerve growth.

References and Notes

1. C. S. Goodman and C. J. Shatz, *Cell* **72/Neuron** 10 (suppl.), 77 (1993).
2. S. B. Kater and L. R. Mills, *J. Neurosci.* **11**, 891 (1991).
3. C. Cypher and P. C. Letourneau, *Curr. Opin. Cell Biol.* **4**, 4 (1992).
4. T. B. Kuhn, C. V. Williams, P. Dou, S. Kater, *J. Neurosci.* **18**, 184 (1998).
5. P. Doherty and F. S. Walsh, *Curr. Opin. Neurobiol.* **4**, 49 (1994).
6. T. M. Gomez, D. M. Snow, P. C. Letourneau, *Neuron* **14**, 1233 (1995).
7. J. Q. Zheng, M. Felder, J. A. Conner, M.-m. Poo, *Nature* **368**, 140 (1994); H.-j. Song, G.-l. Ming, M.-m. Poo, *ibid.* **388**, 275 (1997).
8. R. A. Silver, A. G. Lamb, S. R. Bolsover, *ibid.* **343**, 751 (1990).
9. N. Maeda, M. Niinobe, Y. Inoue, K. Mikoshiba, *Dev. Biol.* **133**, 67 (1989); T. Furuichi *et al.*, *Receptors Channels* **1**, 11 (1993); T. Furuichi *et al.*, *Nature* **342**, 32 (1989).
10. Microsome membrane fractions were prepared from DRGs and cerebella of embryonic day (ED) 11 chick embryos or postnatal day (PD) 20 mice, as described (23). Proteins in the microsome fraction (10  $\mu$ g) were subjected to SDS-polyacrylamide gel electrophoresis (5% gel) in the buffer system of U. K. Laemmli [*Nature* **227**, 680 (1970)]. After electrophoretic transfer to polyvinylidene fluoride membranes (Millipore), immunodetection probed with 4C11 mAb (1  $\mu$ g/ml) was carried out and then visualized with an enhanced chemifluorescence immunoblotting kit (Amersham).
11. DRG neurons from ED11 chick embryos were dissociated by trypsinization and cultured on poly-L-lysine- and laminin (Gibco-BRL)-coated cover slips with nerve growth factor-containing L-15 medium (Gibco-BRL) (27). The cells were cultured for 2 hours and fixed with 4% paraformaldehyde in phosphate-buffered saline for 30 min. Indirect immunocytochemistry was done as modified from P. C. Letourneau and T. A. Shattuck [*Development* **105**, 505 (1989)].
12. O. Thastrup *et al.*, *Proc. Natl. Acad. Sci. U.S.A.* **87**, 2466 (1990).
13. TG (10  $\mu$ M) or LiCl (50 mM) dissolved in the culture medium was added at the time of plating. The culture medium (vehicle) and 50 mM of NaCl dissolved in the medium were used for controls in the TG and LiCl experiments, respectively. DRG neurons were treated with these drugs for 2 or 4 hours. At the indicated time points, multiple visual fields ( $n > 5$ ) were chosen at random from replicate cultures and were observed under a phase-contrast microscope (Axiovert 135; Carl Zeiss). The lengths of the longest neurite per cell were measured and analyzed ( $n >$

- 300 cells in a dish) for each condition and at each time point with IPLab Spectrum imaging software (Signal Analytics).
14. Heparin or de-N-sulfated heparin (Sigma) dissolved in culture medium (1.6 mg/ml) was loaded into DRG neurons by trituration. The trituration loading was confirmed by observing fluorescence of FITC-conjugated dextran (molecular size: 150 kD; Sigma) coincidentally loaded with the test reagents.
15. M. J. Berridge, C. P. Downes, M. R. Hanley, *Cell* **59**, 411 (1989).
16. Heparin or de-N-sulfated heparin (1.6 mg/ml in pipette) was microinjected into cultured DRG neurons with neurites and growth cones. Microinjected test reagents were confirmed by observing the fluorescence of FITC concomitantly injected. Growth cone behavior was observed by time-lapse video microscopy with a cooled charge-coupled device (CCD) camera (PXL-1400; Photometrics) and a Macintosh computer with IPLab Spectrum imaging software.
17. D. G. Jay and H. Keshishian, *Nature* **348**, 548 (1990).
18. J. C. Liao, J. Roeder, D. G. Jay, *Proc. Natl. Acad. Sci. U.S.A.* **91**, 2659 (1994).
19. H. Y. Chang *et al.*, *Nature* **376**, 686 (1995).
20. F.-S. Wang *et al.*, *Science* **273**, 660 (1996).
21. A. M. Sydor *et al.*, *J. Cell Biol.* **134**, 1197 (1996).
22. Microsome membrane fractions were prepared from cerebella of adult mice, as described (23). The 4C11 mAb and the nonspecific IgG (Chemicon International) were labeled with malachite green isothiocyanate (MG) (Molecular Probes) [D. G. Jay, *Proc. Natl. Acad. Sci. U.S.A.* **85**, 5454 (1988)]. Proteins (0.4 mg/ml) in the microsome fraction dissolved in a  $Ca^{2+}$  mobilization buffer were incubated with either MG-labeled 4C11 mAb (20  $\mu$ g/ml) or MG-labeled nonspecific IgG (20  $\mu$ g/ml) for 30 min and then subjected to laser irradiation (10 min, wavelength  $\lambda = 620$  nm, line length  $\tau = 8.0$  ns,  $5 \pm 1$  mJ) per pulse at 10 Hz, 1.5-mm diameter), from a pulsed neodymium:yttrium-aluminum-garnet pump laser (Quanta-Ray, GCR-230-10; Spectra-Physics) and optical parametric oscillator (MOPO-730; Spectra-Physics). IICR measurement was done as described (23). Samples were incubated at 30°C in a buffer containing 1.0 mM adenosine triphosphate (ATP) and an ATP regeneration system, and  $Ca^{2+}$  uptake by ATP and release by  $IP_3$  (200 nM) activities were monitored with calcium green-1 (2  $\mu$ M) (Molecular Probes) in a luminescence spectrometer (LS50B; Perkin-Elmer). The  $Ca^{2+}$  concentration in the buffer was calculated from the maximal fluorescence value ( $F_{max}$ ) and minimum flu-

- orescence value ( $F_{min}$ ) obtained in the presence of excess  $Ca^{2+}$  (100  $\mu$ M of  $CaCl_2$ ) and 10 mM of ethylene glycol-bis( $\beta$ -aminoethyl ether)-*N,N,N',N'*-tetraacetic acid, respectively, after treatment with ionomycin (10  $\mu$ M). The equation used was  $[Ca^{2+}] = K_d(F - F_{min}) / (F_{max} - F)$ , where  $K_d$  is the rate constant of fluorescence dye.
23. S. Nakade, N. Maeda, K. Mikoshiba, *Biochem. J.* **277**, 125 (1991).
24. The MG-labeled antibodies (1.0 mg/ml) were loaded by trituration, as described (19-21). MG-labeled nonspecific rat or mouse IgG (Chemicon International) was used for control experiments. Micro-CALI experiments were done within 10 hours after antibody loading. Some experiments in each micro-CALI experiment were analyzed in a blind fashion to verify the results of analysis ( $n = 18$ ). DRG neuronal cultures were kept at 37°C in a stage incubator throughout the experiment. Complete retention of the loaded antibodies within the growth cone was confirmed for 10 hours after antibody loading in about 82% of FITC-positive cells, by immunocytochemistry with a secondary antibody in the same FITC-positive cells. A chosen growth cone was observed with phase-contrast optics with a  $\times 40$  objective lens (Plan-Neofluar; Carl Zeiss) for 5 min, and then a region of the growth cone was subjected to laser irradiation (5 min,  $\lambda = 620$  nm,  $\tau = 3.5$  ns, 20  $\mu$ J per pulse at 20 Hz, about 14- $\mu$ m diameter), with a nitrogen-driven dye laser (VSL-337ND and DLMS-220; Laser Science). Growth cones were observed during irradiation and, for an additional 15 min, by time-lapse video microscopy (every 10 s) with a cooled CCD camera (PXL-1400; Photometrics) and a Macintosh computer with a custom-made software TI-Workbench written by T. Inoue.
25. K. Takei *et al.*, unpublished data.
26. M. F. A. VanBerkum and C. S. Goodman, *Neuron* **14**, 43 (1995).
27. Y. Goshima, S. Ohsako, T. Yamauchi, *J. Neurosci.* **13**, 559 (1993).
28. Y. Aihara *et al.*, unpublished data.
29. M. Matsumoto *et al.*, *Nature* **379**, 168 (1996).
30. We thank T. Michikawa, A. Muto, H. Mizuno, A. Doi, W. Saikawa, R. Ando, A. Takahashi, and W. Cai for technical assistance and Y. Goshima and M. Ohara for critical reading of the manuscript. Supported by grants from Japan Science and Technology Agency.

19 June 1998; accepted 27 October 1998

## Cultural Selection and Genetic Diversity in Matrilineal Whales

Hal Whitehead

Low diversities of mitochondrial DNA (mtDNA) have recently been found in four species of matrilineal whale. No satisfactory explanation for this apparent anomaly has been previously suggested. Culture seems to be an important part of the lives of matrilineal whales. The selection of matrilineally transmitted cultural traits, upon which neutral mtDNA alleles "hitchhike," has the potential to strongly reduce genetic variation. Thus, in contrast to other nonhuman mammals, culture may be an important evolutionary force for the matrilineal whales.

Most female pilot whales (*Globicephala melas* and *G. macrorhynchus*), sperm whales (*Physeter macrocephalus*), and killer whales (*Orcinus orca*) spend their entire lives with

close female relatives, form new groups primarily by group fission, and so have a social structure that may be called matrilineal (1). These toothed whale (suborder Odontoceti) species have mtDNA nucleotide diversities about tenfold lower than is estimated for other whales and dolphins, with the exception of the narwhal (*Monodon monoceros*) (Table

Department of Biology, Dalhousie University, Halifax, Nova Scotia, Canada B3H 4J1. E-mail: hwhiteh@is.dal.ca